Published by Nigerian Society of Physical Sciences. Hosted by FLAYOO Publishing House LTD

Proceedings of the Nigerian Society of Physical Sciences

Journal Homepage: https://flayoophl.com/journals/index.php/pnspsc

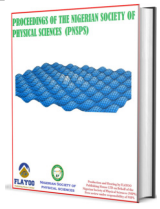

Chemostratigraphy and paleoenvironmental analysis of sand-shale formations using core geochemical spectroscopy tools

Oluwakemi Efemena[a,*], Franklin Lucas[b]

[a]*Department of Geological Sciences, Achievers University, Owo, Ondo State, Nigeria*
[b]*Department of Geology, University of Benin, Benin City, Nigeria*

ABSTRACT

Modern investigations into spectral gamma-ray (SGR) records enhance understanding of sedimentary environments and paleoenvironmental conditions. This study examines a 111 m sand and shale interval in the Tak-1 well, Niger Delta Basin, to characterize clay mineral types and interpret depositional settings. The evaluation of lithology, mineral composition, and geochemical properties through core slabs investigation and spectroscopic analysis revealed information about depositional settings. Spectroscopic analysis of spectral gamma-ray data identified key elements—potassium (K), uranium (U), and thorium (Th)—to differentiate clay minerals, correlate chemostratigraphy, and reconstruct paleoenvironments. Results show that the lithology consists predominantly of sandstone, with occasional interbedding of shaly sand and sandy shale. Uranium and thorium are abundant in mudrocks, while feldspars, micas, and glauconite dominate sandstones. Th/K ratio cross-plots identified smectite/mixed-layer clays, with low Th/K values indicating potassium-rich minerals such as illite, mica, or feldspar. Sandstones contained potassium-bearing minerals like glauconite and evaporites. High uranium values (10–15 ppm) and low Th/U ratios signified organic-rich source rocks formed under anoxic, reducing conditions. Extremely low potassium values (<2%) indicated terrestrial sandstone deposits rich in feldspar. These geochemical and mineralogical characteristics suggest a transitional depositional environment influenced by both terrestrial and marginal marine settings. Fluctuating sea levels shaped sedimentation, with the study interval primarily reflecting a marine paralic anoxic setting with intermittent deltaic influence.

Keywords: Clay minerals, Anoxic reducing environments, Spectral gamma-ray (SGR), Depositional settings, Niger-Delta basin.

DOI:10.61298/pnspsc.2025.2.167

1. INTRODUCTION

The Tak-1 well is located in a hydrocarbon exploration block, approximately 14 km south of Assa North, in the northern part of the Niger Delta. Given its myriad hydrocarbon-bearing reservoirs associated with a complex depositional system, this field is of high interest. Just the Niger Delta is a world-class hydrocarbon province that has developed as a result of fluvial, deltaic, and marine processes since the Late Cretaceous [1]. In the studied field, the reservoirs are largely contained within deep marine and marine paralic sequences, indicating a dynamic depositional environment controlled by changes in sea-level and sediment input [2]. Similar to types of deep marine deposits consisting of

*Corresponding Author Tel. No.: +234-803-9138-949.
e-mail: onomeefe01@yahoo.com (Oluwakemi Efemena)

turbidite sandstones, the geologic time limits a sandstone class of excellent reservoirs of hydrocarbons, mainly due to their high porosity and permeability. Such turbidites, deposited by submarine flows that were driven by gravity, associated channelized and lobated sand bodies [3]. In contrast, the paralic sequences deposited in marine environments reflect a continuum between completely marine and fully continental environments, containing interbedded sandstone, shales, and coals. Such paralic deposits are related to delta-front and shoreface settings, generating a vital component of hydrocarbon migration and trapping [4]. To maximize hydrocarbon exploration and production in this geologically complicated area, it is crucial to comprehend the stratigraphic framework and reservoir architecture of the field.

In the Niger Delta region, the stratigraphy of subsurface structures predominantly comprises repeating sequences of finely layered sediments, primarily alternating sandstones and shales. These sedimentary successions are indicative of the interplay of fluvial, deltaic, and marine depositional environments driven by eustatic sea-level changes and sediment supply dynamics [5]. These cycles of sand and shale deposition are a consequence of progradational and retrogradational phases of the deltaic system that have played a role since the Late Cretaceous. Due to their high porosity and permeability, the sand-dominated units usually reflect high-energy environments such shoreface settings and distributary channels, offering good reservoir quality. Conversely, the interbedded shales serve as source rocks and regional seals, creating efficient hydrocarbon traps [6]. Additionally, syn-depositional faulting and compactional processes alter reservoir continuity and hydrocarbon migration paths, contributing to the heterolithic structure of these strata.

The Niger Delta's sand-shale alternations must be thoroughly understood to properly characterize reservoirs, site wells, and optimize hydrocarbon recovery [7]. In this intricate depositional system, geoscientists may more accurately define reservoir geometries and forecast fluid flow behavior by combining seismic, well-log, and core data. Assessing the types of clay minerals found in subsurface formations is essential to comprehending diagenetic processes, reservoir quality, and depositional environments. To differentiate between various clay minerals and evaporites using spectral gamma-ray data, a variety of graphical methods and cross-plots are frequently used.

Plots of potassium (K), thorium (Th), and uranium (U) elemental concentrations are frequently used to illustrate the theoretical distribution of clay minerals and evaporites. Mineralogical changes can be inferred from the different quantities of radioactive elements found in different clay minerals. For example, kaolinite has low potassium but comparatively high thorium concentrations, while illite and glauconite are rich in potassium. Conversely, smectite has moderate potassium content, although the concentration of thorium varies based on diagenetic changes [8]. In spectral gamma-ray logs, evaporites like anhydrite and halite may be distinguished since they usually have very little radioactivity. Dominating clay minerals are determined based on a cross-plot of thorium to potassium, ranging from potassium-bearing evaporites: < 0.06, Glauconite: 0.6-1.5, Kaolinite: 1.5-2.0, Micas: 1.5-2.0 illite 2-3.5 and Mixed-layered: > 3.5 [8].

A thorough investigation of chemostratigraphy and paleoenvironmental analysis of sand-shale formations using core geochemical spectroscopy tools is presented in this paper. Chemostratigraphy enables the differentiation and correlation of stratigraphic units by analyzing the elemental composition of sedimentary sequences, offering insights into diagenetic processes and depositional environments. This method helps create more accurate geological models and improves our comprehension of reservoir heterogeneity. The resolution and accuracy of these analyses have been enhanced by recent developments in geochemical logging methods, allowing for more thorough characterizations of intricate formations. Herron's geochemical classification system for terrigenous sands and shales, for example, has proven crucial in improving stratigraphic interpretations [9]. To provide a more nuanced understanding of the stratigraphic architecture and paleoenvironmental conditions of the study area, our research attempts to expand upon these approaches.

2. DESCRIPTIVE AND GEOSTATISTICAL METHOD

Core slabs of the six core runs were examined for their lithological diversity and stratigraphic significance. To physically examine core slabs, lithological boundaries and sedimentary features were identified by meticulous scrutiny in the core storage and laboratory [10]. Recording visual features facilitated further analysis, and high-resolution photos of every core slab captured were provided and examined in the laboratory. These pictures were crucial resources for identifying sedimentary features and lithological correlations [11]. Important stratigraphic markers and sedimentary textures were identified. Spectral gamma ray logs were utilized to detect changes in radioactive elements that are indicative of clay mineral composition and sedimentary facies, such as potassium (K), uranium (U), and thorium (Th), helping to delineate depositional environments and lithological boundaries [12].

For assessing clay mineralogy and interpreting sedimentary facies, graphic distribution analysis and cross-plot techniques are useful. When combined with spectral gamma-ray log interpretation, the Th/K and Th/U cross-plots improve the understanding of clay mineral composition and depositional environments in hydrocarbon reservoirs (Figure 1).

2.1. THORIUM TO POTASSIUM (TH/K) CROSS-PLOT

High potassium (K) and low thorium (Th) values typically indicate the presence of illite and glauconite, high thorium and low potassium values suggest a dominance of kaolinite while smectite and mixed-layer clays fall somewhere in the middle of these two extremes [12].

2.2. THORIUM TO URANIUM (TH/U) RATIO

The Th/U ratio is useful for distinguishing depositional redox conditions and clay types. A high Th/U ratio (>7) suggests oxidizing conditions, which favour kaolinite and other detrital clays, whereas a low Th/U ratio (<2) may indicate reducing environments, that lacks oxygen, where organic matter and uranium enrichment occur. However, in environments where oxygen availability fluctuates, leading to a mix of clay minerals such as illite, smectite, and glauconite, the Th/U ratio typically falls within the intermediate range (2–7), representing transitional settings [13].

Table 1. Core description and gamma spectroscopy analyses.

Core#	Depth meter	Lithofacies	Total Gamma API	Potassium %	Uranium ppm	Thorium ppm	Uranium-Free ppm	Th/K ppm/%	Th/U ppm
	3041.00	Sandstone	14	2.0	2.8	0.3	11.19	0.17	0.12
	3042.00	Sandstone	18.2	1.1	1.43	2.45	16.72	2.30	1.71
	3043.80	Sandstone	41	3.1	8.2	0	32.65	0.00	0.00
1	3045.00	Sandstone	30	2.1	2.2	3.2	28.07	1.52	1.44
	3050.00	Sandstone	17	2.2	2.2	0.03	14.64	0.01	0.01
	3055.00	Sandstone	18	1.1	2.3	0.03	16.01	0.03	0.01
	3059.63	Sandstone	26	1.9	1.6	0.09	23.92	0.05	0.06
	3060.00	Sandstone	71	4.8	10.8	3.0	60.29	0.62	0.27
	3065.00	Sandstone	22	2.3	2.8	0.5	19.06	0.23	0.19
2	3067.00	Sandstone	26	1.6	1.2	1.08	24.95	0.70	0.89
	3070.00	Sandstone	30	2.4	3.6	1.1	26.45	0.44	0.30
	3075.00	Sandstone	46	4.9	3.3	2.2	42.90	0.46	0.67
	3077.95	Sandstone	20	1.2	4.6	0.09	15.60	0.08	0.02
	3080.00	Sandstone	33	2.7	3.6	2.5	29.89	0.93	0.69
	3085.00	Sandstone	24	1.4	3.6	0.3	20.79	0.18	0.07
3	3087.00	Sandstone	76	5.2	10.8	0.3	65.33	0.06	0.03
	3090.00	Sandstone	22	1.5	3.7	1.6	18.09	1.04	0.4
	3095.00	Sandstone	21	1.5	2.1	1.1	18.52	0.69	0.5
	3096.00	Sandstone	16	1.2	0.46	1.8	15.95	1.46	3.75
	3096.75	Sandstone	24	3.4	4.1	0.03	19.83	0.01	0.01
	3100.00	Sandstone	25	2.3	5.2	0.4	19.58	0.17	0.07
	3105.00	Sandstone	28	2.6	2.7	1.3	24.80	0.51	0.47
4	3107.33	Shaly sand	85.5	5.9	12.79	2.72	72.70	0.46	0.21
	3110.00	Sandstone	47	3.6	6.7	2.5	40.73	0.69	0.37
	3113.85	Sandstone	19.4	2.31	0.81	0.03	18.68	0.01	0.04
	3115.00	Sandstone	28	1.9	5.0	1.1	22.92	0.55	0.21
	3115.30	Sandstone	23	2.4	2.5	0.04	20.73	0.02	0.02
	3120.00	Sandstone	27	1.6	4.7	0.0	22.60	0.00	0.00
	3125.00	Sandstone	24	1.7	3.3	0.03	20.78	0.02	0.01
5	3127.11	Sandstone	23.30	2.53	1.19	1.50	22.11	0.59	1.26
	3130.00	Sandstone	15	1.3	2.7	0.8	12.19	0.63	0.30
	3132.57	Sandstone	63.3	4.35	9.81	4.82	53.46	1.11	0.49
	3133.75	Sandstone	33	2.3	3.5	1.3	29.45	0.56	0.37
	3135.00	Sandstone	59	5.3	6.7	1.0	51.99	0.19	0.15
	3137.42	Sandy shale	109.57	7.2	14.66	5.06	94.91	0.70	0.35
6	3140.00	Shaly sand	85	5.3	7.9	0.8	77.40	0.15	0.10
	3145.00	Sandstone	62	6.2	5.7	2.0	55.87	0.33	0.35
	3150.00	Sandstone	20	2.5	3.8	0.9	16.22	0.34	0.22
	3152.00	Sandstone	35	2.7	3.1	2.9	32.01	1.06	0.94

3. RESULTS AND DISCUSSION

The description of the cores and spectral gamma log delineation revealed the results presented in Table 1. Sandstone with concretions, which are light grey, fine-grained, well-sorted, well-cemented, and highly bioturbated, with muddy heteroliths and ichnogenera like Thalassinoides, Chondrites, and Palaeophycus, make up the majority of the examined interval. Light to dark brown is the range of colors for the sandstone, which has fine to medium-sized grains that are moderately to well-sorted. At the mid-level, Ophiomorpha predominates and the grain size increases to coarse and pebbly, with poorly sorted pebbles and considerable bioturbation. In addition, the interval (3388.00m–3388.35m) has sandy shale and shale, with fine-grained sandstone and shale lamination that is highly bioturbated by Ophiomorpha. Furthermore, the presence of fine to coarse pebbly grains with discernible laminations in intercalated sandstone and shale suggests a dynamic depositional environment of marine setting [14].

The spectral gamma-ray analysis (Table 1 and Figure 2) provided insights into the distribution of potassium (K), uranium (U), and thorium (Th), which are key indicators of lithology and depositional environments for paleoenvironmental reconstruction. The given data's gamma-ray values, represent lithological diversity, range from 14 to 109.57 API units (Figure 2). Cleaner sandstone deposits with less shale are generally indicated by lower gamma-ray values, which are an indicator of high reser-

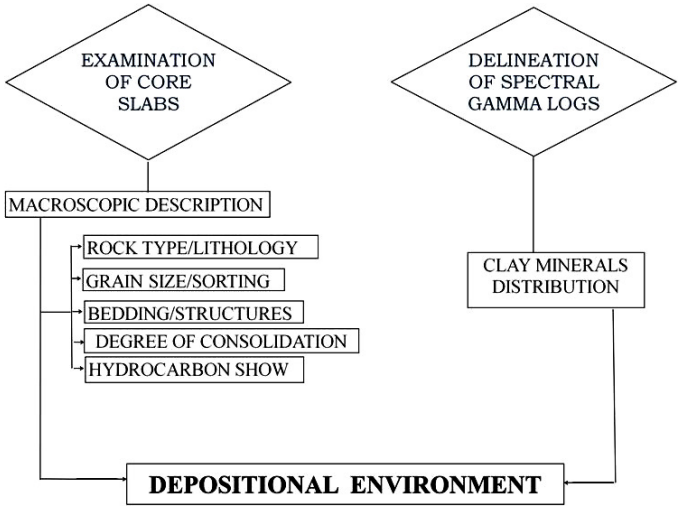

Figure 1. Methodology flow chart.

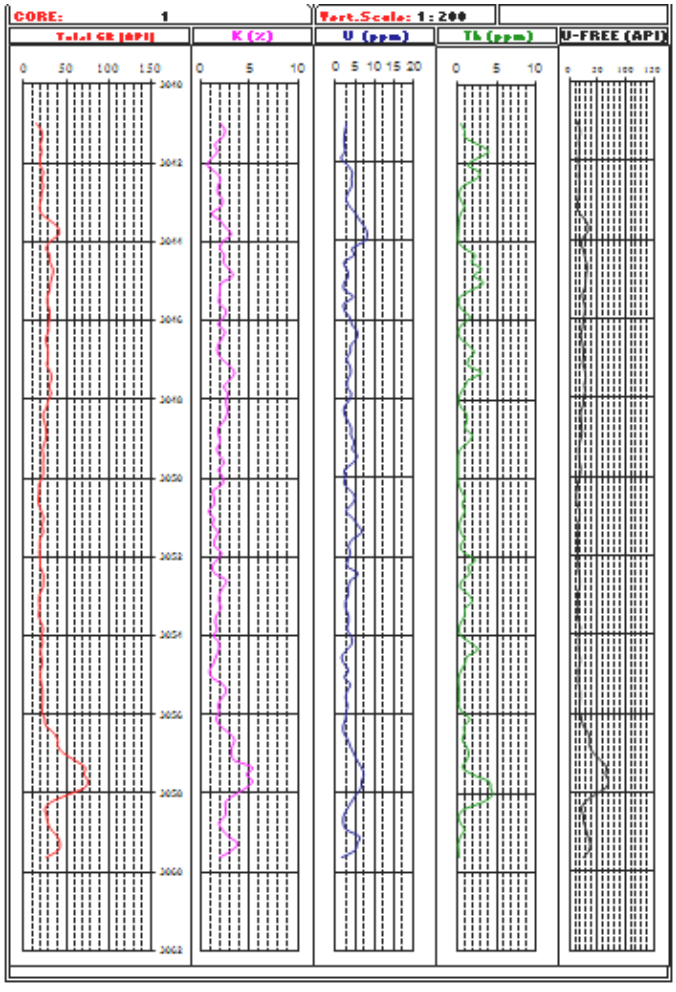

Figure 2. Spectral Gamma Log showing GR (API), K (%), U(ppm) and Th (ppm).

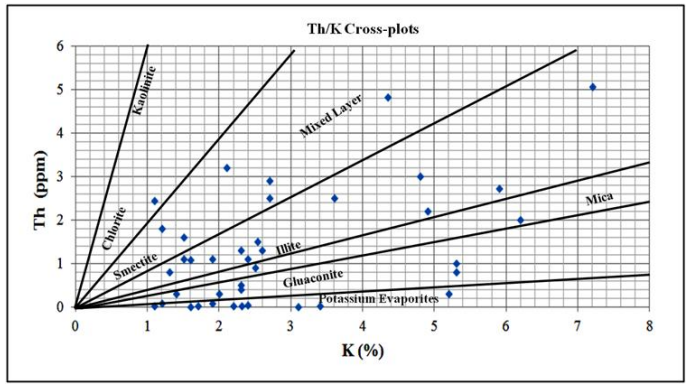

Figure 3. Schematic graph of clay mineral distribution and evaporates [18].

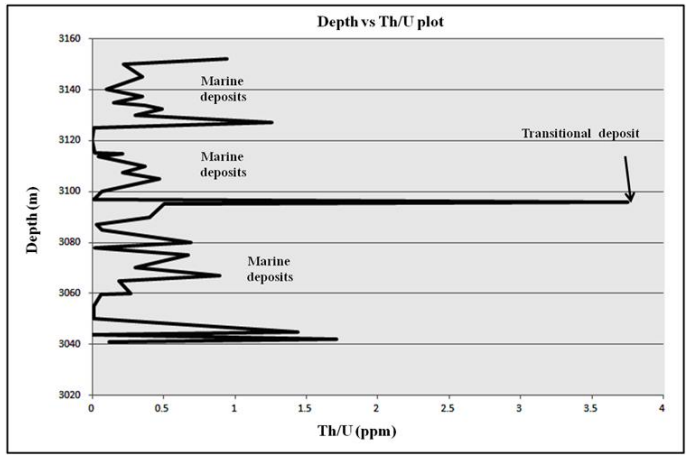

Figure 4. Interpretation of Th/U ratio for depositional environment [24].

voir quality [15]. Higher shale content, on the other hand, is suggested by higher gamma-ray values (up to 109.57 API in core #6 at 3137.42 m). This suggests that there may be more clay minerals, less permeability, and maybe organic-rich intervals that could act as hydrocarbon source rocks instead of reservoirs.

Concentrations of potassium (K) in the examined core samples range from 1.1% to 7.2%, with the majority of results falling below 3%. Periods with lower potassium contents are characterized by quartz-rich sandstones, carbonates, or organic-rich shales, where core slabs show a predominance of quartz in the rock matrix. Because there are no minerals that contain potassium, these settings naturally exhibit low potassium levels. Conversely, higher potassium levels (up to 7.2%) indicate an environment rich in clay, which is typical of deeper marine or lagoonal environments with fine-grained sediments [16]. Uranium (U) concentrations in the analyzed core samples range from 0.46 ppm to 14.66 ppm, with notable variations across different depths. The highest uranium value (14.66 ppm) occurs at 3137.42 m, while other notable peaks include 12.79 ppm at 3107.33 m, 10.8 ppm at 3060.00 m/3087.00 m, and 9.81 ppm at 3132.00 m. These peaks coincide with moderate potassium and thorium levels. The lowest uranium content (0.46 ppm) is observed at 3096.00 m, where potassium is also very low (1.2%) and thorium is relatively high (1.8 ppm) [12]. Thorium (Th) concentrations in the analyzed core samples range from 1.2 ppm to 14.6 ppm, with notable differences observed across various depths. Thorium values are generally low across all cores, ranging from 0.0 to 3.2 ppm, indicating a predominance of sand-rich facies with limited heavy mineral enrichment. Higher thorium values (2.5–3.2 ppm) cor-

relate with increased gamma activity and potassium levels, suggesting the presence of shale or clay-rich layers, likely interbedded within sandstones [17].

There are wide ranges of clay mineral groups present in the examined cores, as indicated by the computed Th/K ratios, which range from 0.00 to 1.52. Feldspathic sediments or evaporites containing potassium are represented by values less than 0.06. Indicating significant diagenesis and maritime effect, glauconite-aligned ratios range from 0.6 to 1.5. Values greater than 1.5 show that kaolinite, mica, or illite—which are typically found in sediments that have seen more extensive weathering or metamorphism—do not significantly dominate the sample [12]. This indicates that the sediments under investigation most likely contain a mixture of feldspars, glauconitic minerals, and some clay-rich components (Figure 2). A depth of 3.75 Th/U suggests a change in the source of the sediment or a shift to more oxidizing circumstances, which could be brought on by variations in sediment influx, elevated ventilation, or sea level fluctuations. In Figure 3, Th/U < 2, most samples, however, show dominantly decreasing circumstances during deposition. Marine shales, deep-sea anoxic basins, and lagoonal environments with limited oxygen availability are common places to find low Th/U ratios (<2) [17].

3.1. TH/K RATIOS AND CLAY MINERAL ANALYSIS INTEGRATION

Low K, and low Th values suggest the presence of illite and glauconite, indicating marine-influenced, reducing conditions with limited terrestrial input. Low Th/K ratios indicate smectite/mixed-layer clays, suggesting deposition in reducing environments with high organic matter, such as marine anoxic basins [12, 17]. The precipitation of potassium salts influences the formation and transformation of clay minerals. High potassium concentrations can lead to the development of illite or illite-smectite mixed-layer clays, as potassium ions become fixed within clay structures during diagenesis [19, 20]. This process results in a clay mineral assemblage dominated by illitic clays, reflecting the availability of potassium from evaporite minerals [21]. The presence of potassium evaporites indicates deposition in arid conditions with high evaporation rates, typically in restricted basins with limited water influx, favoring the concentration and precipitation of soluble salts [22]. The associated clay minerals, particularly illite, suggest minimal chemical weathering and a detrital input from areas dominated by physical weathering, aligning with arid to semi-arid climatic conditions [23]. Therefore, the combined presence of potassium evaporites and specific clay mineral assemblages serves as a strong indicator of past arid climatic conditions and restricted depositional environments.

3.2. CORRELATION OF TH/U AND TH/K RATIOS FOR ENHANCED DEPOSITIONAL INTERPRETATION

The depositional environments were deduced to be anoxic, based on a low Th/U ratio (<2) combined with low K values, which support a smectite-dominated environment. This reflects a high organic matter accumulation zone with reducing conditions. Fluctuating redox conditions were observed at a depth of 3096.00 m, suggesting an illite-rich, glauconite environment indicative of moderate weathering and an estuarine or shallow marine setting (Figure 4)

4. CONCLUSION

Integrating core descriptions with spectral gamma-ray data, the results show that dark brown to dark gray sandstone predominates. It has quartz, fine to coarse grains with pebbles, and shows changes in the concentrations of uranium (U), thorium (Th), and potassium (K). Rebuilding the depositional environment and stratigraphic distinction depend on these variances. Cleaner sandstone formations with less shale and periods with more clay material presence have been compared by the gamma-ray trends [25]. These results are consistent with earlier research by Refs. [26] and [27] that link stratigraphic differentiation and reservoir quality to gamma-ray signals. Although there are sporadic clay-rich intervals that indicate localized modifications in depositional settings, the detected potassium values further substantiate the occurrence of quartz-rich sandstones. According to Ref. [28], core slab measurements support this hypothesis by showing a matrix of rock that is dominated by quartz with trace amounts of feldspathic contributions.

Variations in the concentrations of uranium and thorium offer further information on the paleoenvironmental circumstances of the period under study. While lower uranium values imply more oxidizing environments, uranium enrichment at particular depths indicates periods of greater organic matter accumulation under reducing conditions [29]. In a similar vein, variations in sediment provenance and diagenetic alterations are reflected in the distribution of thorium concentrations, which lends support to the idea of alternating sand-rich and shale-dominated facies [30]. The determined Th/K ratios highlight the formation's mineralogical complexity even further, suggesting a dynamic depositional system impacted by both terrestrial and marine sources [31]. The presence of glauconitic minerals, as inferred from Th/K ratios, further indicates marine influences and diagenetic modifications that may have impacted sediment composition and reservoir properties. When taken as a whole, these geochemical markers help to clarify the depositional setting of the sequence under study.

A notable shift in redox conditions is inferred from the Th/U ratio variations. One depth, exhibiting a Th/U ratio of 3.75, suggests oxidizing conditions potentially linked to sea-level fluctuations, enhanced ventilation, or shifts in sediment influx [24]. However, the majority of the samples display Th/U ratios below 2, signifying predominantly reducing conditions during deposition. Such low Th/U values are characteristic of marine shales, deep-sea anoxic basins, or lagoonal settings with restricted oxygen availability [32, 33], reinforcing the interpretation of a depositional environment dominated by low-oxygen conditions. The paleoenvironment suggests shifting depositional circumstances and sea-level fluctuations, with a mostly deep-marine anoxic setting and infrequent deltaic influence.

DATA AVAILABILITY

The data used in this study are available upon reasonable request from the corresponding author.

References

[1] H. Doust & E. Omatsola, ''Niger Delta,'' in *Divergent/Passive Margin Basins*, J. D. Edwards, P. A. Santogrossi (Eds.), AAPG Memoir 48, American Association of Petroleum Geologists, Tulsa, OK, 1990, pp. 201–238. [Online]. https://doi.org/10.1306/M48508C4.

[2] K. C. Short & A. J. Stauble, ''Outline of geology of Niger Delta'', American Association of Petroleum Geologists Bulletin **51** (1967) 761. https://archives.datapages.com/data/bulletns/1965-67/data/pg/0051/0005/0750/0761.htm.

[3] B. D. Evamy, J. Haremboure, P. Kamerling, W. A. Knaap, F. A. Molloy & P. H. Rowlands, ''Hydrocarbon habitat of Tertiary Niger Delta,'' American Association of Petroleum Geologists Bulletin **62** (1978) 1. https://doi.org/10.1306/C1EA47ED-16C9-11D7-8645000102C1865D.

[4] T. J. A. Reijers, ''Stratigraphy and sedimentology of the Niger Delta'', Geologos **17** (2011) 133. https://sciendo.com/article/10.2478/v10118-011-0008-3.

[5] T. J. A. Reijers, S. W. Petters & C. S. Nwajide, ''The Niger Delta basin'', in *Sedimentary Basins of the World*, R. C. Selley (Ed.), Elsevier, Volume 3, 1997, pp. 151–172. https://doi.org/10.1016/S1874-5997(97)80010-X

[6] N. G. Obaje, ''Geology and mineral resources of Nigeria'', Developments in Petroleum Science **57** (2013) 221. https://doi.org/10.1007/978-3-540-92685-6.

[7] I. O. Ibrahim, B. D. Ibrahim, C. S. Ngozi-Chika, A. S. Adeoye & S. Shaibu, ''Hydrocarbon prospectivity of selected block wells, Southern Niger Delta, Nigeria'', Discovery Nature **1** (2024) e1dn1003. https://doi.org/10.54905/disssi.v1i1.e1dn1003.

[8] J. Klaja & L. Dudek, ''Geological interpretation of spectral gamma ray (SGR) logging in selected boreholes'', Nafta-Gaz **72** (2016) 3. http://dx.doi.org/10.18668/ng2016.01.01.

[9] M. M. Herron, ''Geochemical classification of terrigenous sands and shales from core or log data'', Journal of Sedimentary Research **58** (1988) 820. https://doi.org/10.1306/212F8E77-2B24-11D7-8648000102C1865D.

[10] C. T. Siemers & R. W. Tillman, ''Recommendations for the proper handling of cores and sedimentological analysis of core sequences'', in *Deep-water clastic sediments: a core workshop*, C. T. Siemers, R. W. Tillman, C. R. Williamson (Eds.), SEPM Society for Sedimentary Geology, 1981, https://doi.org/10.2110/cor.81.01.0020.

[11] M. S. Erenpreiss, ''High-resolution core photography and spectral gamma-ray logging'', *A geologic play book for Utica Shale Appalachian basin exploration*, D. G. Patchen & K. M. Carter (Eds.), Final report of the Utica Shale Appalachian basin exploration consortium, 2015, pp. 36–49. [Online]. Available from: http://www.wvgs.wvnet.edu/utica.

[12] M. Rider, *The Geological Interpretation of Well Logs*, Gulf Publishing Company, 1996. [Online]. https://archive.org/details/geologicalinterp0000ride.

[13] O. Serra, ''The interpretation of logging data'', 1986. [Online]. https://www.scribd.com/document/391792483/O-Serra-the-Interpretation-of-Logging-Data-1986.

[14] R. G. Rothwell & F. Rack, ''New techniques in sediment core analysis: An introduction'', Geological Society London Special Publications, **267** (2006) 1. https://doi.org/10.1144/GSL.SP.2006.267.01.01.

[15] G. Asquith & D. Krygowski, ''Basic well log analysis'', in *Methods in exploration*, American Association of Petroleum Geologists, Tulsa, 2004, pp. 31–34. https://doi.org/10.1306/Mth16823.

[16] Y. Guan, Y. Chen, X. Sun, L. Xu, D. Xu, Z. Zhu & W. He, ''The clay mineralogy and geochemistry of sediments in the beibu gulf, South Xhina sea: a record of the holocene sedimentary environmental change'', Journal of Marine Science and Engineering **11** (2023) 1463. https://doi.org/10.3390/jmse11071463.

[17] B. L. Dickson & K. M. Scott, ''Interpretation of aerial gamma-ray surveys—adding the geochemical factors'', Australian Geological Survey Organisation Journal of Australian Geology & Geophysics **17** (1997) 187. https://www.osti.gov/etdeweb/biblio/499122.

[18] Schlumberger, *Log interpretation charts*, 2013. [Online]. https://www.spec2000.net/downloads/SLB%20Chartbook%202013.pdf.

[19] J. J. Howard, ''Lithium and potassium saturation of illite/smectite clays from interlaminated shales and sandstones'', Clays and Clay Minerals **29** (1981) 136. https://doi.org/10.1346/CCMN.1981.0290208.

[20] G. Yuan, Y. Cao, H. M. Schulz, F. Hao, J. Gluyas, K. Liu, T. Yang, Y. Wang, K. Xi & F. Li, ''A review of feldspar alteration and its geological significance in sedimentary basins: from shallow aquifers to deep hydrocarbon reservoirs'', Earth-Science Reviews **191** (2019) 114. https://doi.org/10.1016/j.earscirev.2019.02.004.

[21] R. L. Hay, S. G. Guldman, J. C. Matthews, R. H. Lander, M. E. Duffin & T. K. Kyser, ''Clay mineral diagenesis in Core KM-3 of Searles lake, California'', Clays and Clay Minerals **39** (1991) 84. https://doi.org/10.1346/CCMN.1991.0390111.

[22] B. Lanson, D. Beaufort, G. Berger, A. Bauer, A. Cassagnabère & A. Meunier, ''Authigenic kaolin and illitic minerals during burial diagenesis of sandstones: a review'', Clay Minerals **37** (2002) 1. https://doi.org/10.1180/0009855023710014.

[23] K. Bjørlykke & P. Aagaard, ''Clay minerals in North Sea sandstones'', in *Origin, Diagenesis, and Petrophysics of Clay Minerals in Sandstones*, SEPM Society for Sedimentary Geology, 1992. https://doi.org/10.2110/pec.92.47.0065.

[24] J. A. S. Adams & C. E. Weaver, ''Thorium-to-Uranium ratios as indicators of sedimentary processes: example of concept of geochemical facies'', American Association of Petroleum Geologists Bulletin **42** (1958) 387. https://doi.org/10.1306/0BDA5A89-16BD-11D7-8645000102C1865D.

[25] C. O. Molua, ''Understanding the gamma ray log and its significance in formation analysis'', Earth Sciences Pakistan (ESP) **8** (2024) 55. http://doi.org/10.26480/esp.02.2024.55.60.

[26] J. Schieber, ''Evidence for high-energy events and shallow-water deposition in the Chattanooga Shale, Tennessee, USA'', Sedimentary Geology **93** (1994) 193. https://api.semanticscholar.org/CorpusID:34870486.

[27] D. E. King, ''Incorporating geological data in well log interpretation'', Geological Society, London, Special Publications **48** (1990) 45. https://www.lyellcollection.org.

[28] A. Dokuz & E. Tanyoluo, ''Geochemical constraints on the provenance, mineral sorting and subaerial weathering of lower Jurassic and upper cretaceous clastic rocks of the Eastern Pontides, Yusufeli (Artvin), NE Turkey'', Turkish Journal of Earth Sciences **15** (2006) 181. https://journals.tubitak.gov.tr/earth/vol15/iss2/4.

[29] K. H. Wedepohl, ''Environmental influences on the chemical composition of shales and clays'', Physics and Chemistry of the Earth **8** (1971) 307. https://doi.org/10.1016/0079-1946(71)90020-6.

[30] J. H. Doveton, ''Geological log interpretation'', SEPM Society for Sedimentary Geology **29** 1994 1. https://doi.org/10.2110/scn.94.29.

[31] K. J. Myers & P. B. Wignall, ''Understanding Jurassic organic-rich mudrocks—new concepts using gamma-ray spectrometry and palaeoecology: examples from the Kimmeridge clay of dorset and the jet rock of Yorkshire'', in *Marine clastic sedimentology*, J. K. Leggett & G. G. Zuffa (Eds.), Springer, Dordrecht, 1987, pp. 172–189. https://doi.org/10.1007/978-94-009-3241-8_9.

[32] A. Ito & R. Wagai, ''Global distribution of clay-size minerals on land surface for biogeochemical and climatological studies'', Scientific Data **4** (2017) 1. https://doi.org/10.1038/sdata.2017.103.

[33] Q. Hu, C. Li, B. Yang, X. Fang, H. Lü & X. Shi, ''Clay mineral distribution characteristics of surface sediments in the South Mid-Atlantic Ridge'', Journal of Oceanology and Limnology **41** (2023) 897. https://doi.org/10.1007/s00343-022-2033-1.